Frequency response data based disturbance observer design applicable to non-minimum phase systems

Xiaoke Wang [1†], Wataru Ohnishi[1], and Takafumi Koseki[1]

[1]Department of Electrical Engineering, The University of Tokyo, Tokyo, Japan
(Tel:+81-3-5841-6676; E-mail:wangxiaoke@koseki.t.u-tokyo.ac.jp;ohnishi@ieee.org;takafumikoseki@ieee.org)

Abstract: Disturbance observer (DOB) has been widely used in industrial field due to it's simplicity and effectiveness in rejecting disturbance. The performance of disturbance observer is greatly influenced by the bandwidth of low pass filter (Q filter). This paper proposes a novel way for optimizing bandwidth of Q filter by considering experimentally obtained frequency response data (FRD) of plant. By transforming all the nonliner constraints into convex constraints, the convex optimisation method can be employed to solve this problem easily. The simulation results verified the feasibility of proposed method and demonstrated that the optimized Q filter can gurantee the disturbance rejection performance.

Keywords: Disturbance observer, Q filter bandwidth, frequency response data, convex optimisation

1. INTRODUCTION

In industrial applications, unavoidable disturbances deteriorate the performance of designed control system. To estimate and compensate the effect of disturbance, disturbance observer has been proposed [1]. As an effective tool, DOB has been used in various applications, such as robot manipulators [2], high-speed positioning stage [3] *etc*. In disturbance observer configuration, Q filter is necessary to guarantee the causality of system and the bandwidth of Q filter is desired to be as high as possible to ensure satisfactory disturbance rejection performance in a wide frequency range. However, the bandwidth of Q filter is limited by system robustness and noise, and thus can not be shaped freely [4]. Moreover, in case of a non-minimum phase plant, internal instability due to unstable zeros sets additional limitation for Q filter design [5].

Various guidelines have been proposed on DOB design. By multiplying a filter to shape the plant into nominal plant, Q filter's bandwidth is increased in [6]. State space representation of plant is used to design Q filter in [7]. Focusing on closed loop instead of inner DOB loop to ensure disturbance attenuation performance and robust stability, Q filter's design was given in [8]. For non-minimum phase plant, from the prospective of system robustness and sensitivity function limitation, the range of Q filter's bandwidth has been given in [5] [9] by using Bode integral theorem and Poisson integral theorem. In [10], a new filter whose parallel connection with the plant becomes minimum phase is designed. Then the conventional DOB configuration procedure is employed for the new system.

The aforementioned methods use the parametric model of plant (transfer function or state space representation identified from FRD) which can present the system dynamics directly. However, since identified parametric model involves model uncertainties, the robustness of DOB can be deteriorated. Therefore, in this paper, direct usage of frequency response data based DOB system design has been explored.

† Xiaoke Wang is the presenter of this paper.

Previous frequency response data based research mainly focuses on designing linearly parameterized fixed order feedback controller by loop shaping method. In [11], authors define margin constraint which is linear with respect to controllers' parameters and obtain controller by linear programming. In [12], non-convex optimization method is employed to derive controller. Convex optimization has been used to compute robust controllers for single-input-single-output systems depicted by frequency response data in [13] which has been applied to specifically design PID controller in [14]-[15], and further extended to multi-input-multi-output case in [16]. Based on this method, Matlab toolbox has been developed in [17].

In this paper, integrating the frequency response data based loop shaping method into DOB design has been researched.

1. DOB system for a non-minimum phase plant is designed based on the frequency response data of plant. The bandwidth of DOB has been optimized by employing FRD based loop shaping optimization method.
2. A general way of deriving convex constraints from original nonlinear constraints which limit the peak value of sensitivity function and complementary sensitivity function was given. By introducing conservatism into optimization, this problem can be changed into convex optimization problem and be solved easily.

Remaining part of this paper is organized as follows. Section 2 provides problem formulation, nonlinear constraints will be derived in this section followed by mathematical transformation to convex constraints in Section 3. Based on the constraints obtained, some simulation results are given in Section 4. This paper ends by giving concluding remarks and future work in Section 5.

2. PROBLEM FORMULATION

In the disturbance observer control system as shown in Fig. 1, P_r and P_n denote real plant and nominal minimum phase plant, defined by FRD and transfer function, respectively. Q represents the to-be-designed filter.

$d, \hat{d}, r, y$ are disturbance external input, estimated disturbance, reference input and output, respectively. The feedback controller C_{fb} is assumed to be given.

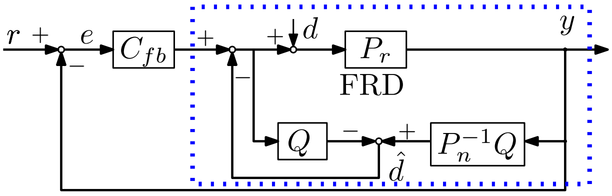

Fig. 1 Block diagram of disturbance observer control system

In this paper, Q is selected as follows in which τ and k are parameters to be decided and the relative order of P_n is 2.

$$Q = \frac{1}{\tau^2 s^2 + 2k\tau s + 1}, \tag{1}$$

then the following equations can be obtained for the blue dotted part in Fig. 1.

$$\begin{aligned} L &= P_n^{-1}Q(1-Q)^{-1}P_r(j\omega) \\ &= \frac{P_r(j\omega)P_n^{-1}}{(s^2\tau^2 + 2k\tau s)} \triangleq \frac{N}{D}, \end{aligned} \tag{2a}$$

$$S = \frac{1}{1 + (1-Q)^{-1}QP_n^{-1}P_r(j\omega)} \triangleq \frac{D}{D+N}, \tag{2b}$$

$$\frac{y}{d} = \frac{P_r(j\omega)}{1 + (1-Q)^{-1}QP_n^{-1}P_r(j\omega)} = SP_r(j\omega), \tag{2c}$$

$$\frac{\hat{d}}{d} = \frac{(1-Q)^{-1}QP_n^{-1}P_r(j\omega)}{1 + (1-Q)^{-1}QP_n^{-1}P_r(j\omega)} = 1 - S = T, \tag{2d}$$

in which $N = P_r(j\omega)P_n^{-1}, D = s^2\tau^2 + 2k\tau s$ and L, S, T represent the open loop function, sensitivity function and complementary sensitivity function, respectively. $j\omega$ means sequential frequency points.

From above equations, to obtain good disturbance rejection performance, the peak value of sensitivity function should be limited and the 0 dB crossover frequency of sensitivity function should be as large as possible. By selecting weighted function for S and T each, the peak value of sensitivity and complementary sensitivity function will be no larger than 2 and 1.25 (commonly used in industrial field). The ω_p and ω_t will be decided by optimization process.

$$W_p = \frac{0.5s + \omega_p}{s}, |W_p S| < 1, \tag{3a}$$

$$W_m = \frac{s + \omega_t}{1.25\omega_t}, \ |W_m T| < 1. \tag{3b}$$

In summary, the problem can be formulated into

$$\begin{aligned} &\underset{\tau,k,\omega_t}{\text{Maximise}} && \omega_p && \text{(4a)} \\ &\text{Subject to} && 0 < \omega_p < \tfrac{1}{\tau} < \omega_t, && \text{(4b)} \\ &&& 0.5 < k < 1, && \text{(4c)} \\ &&& |W_p S| < 1, && \text{(4d)} \\ &&& |W_m T| < 1. && \text{(4e)} \end{aligned}$$

For nonlinear constraints in terms of optimization variables, in next section, transformation to convex constraints will be given.

3. MATHEMATICAL TRANSFORMATION OF NONLINEAR CONSTRAINTS

In this section, the nonlinear constraints are all transformed into linear function or Linear Matrix Inequality (LMI) form of variables $\tau, k, \omega_s, \omega_t$ which can simplify the problem significantly.

3.1. Preliminary

Schur Complement has been used throughout the paper which is introduced as follows where A, B, C, D are scalars or matrices and B^* is the conjugate transpose of B.

$$\begin{bmatrix} A & B \\ B^* & D \end{bmatrix} > 0 \Leftrightarrow A > 0, A - BD^{-1}B^* > 0. \tag{5}$$

Besides, linear approximation is extensively applied to the following section. The basic concept is to estimate the value of a function, $f(x)$, near a point x_0, using the following formula in which $f'(x_0)$ means the slope of the tangent line at x_0.

$$f(x) \approx f(x_0) + f'(x_0)(x - x_0) \tag{6}$$

Additionally, $|A|$ denotes the magnitude of A in which A is a function.

3.2. Constraint Eq. (4b)

For the left side of Eq.(4b), since $\frac{1}{\tau_i}$ is a convex function, linear approximation can be directly used. The approximated value is always smaller than the original one, therefore, if the new inequality holds, the original one must be satisfied.

$$\frac{1}{\tau_i} \geq \frac{-\tau_i}{\tau_{i-1}^2} + \frac{2}{\tau_{i-1}}, \tag{7}$$

in which τ_i means the current value while τ_{i-1} means the previous value in the optimization loop ($\tau_{i-1} > \tau_i$).

Therefore, the original constraint can be changed into following form.

$$0 < \omega_p < \frac{-\tau_i}{\tau_{i-1}^2} + \frac{2}{\tau_{i-1}}. \tag{8}$$

By using Schur Complement, the right side of Eq. (4b) can be rewritten as the following LMI form.

$$\frac{1}{\tau} < \omega_t \Leftrightarrow \begin{bmatrix} \omega_t & 1 \\ 1 & \tau \end{bmatrix} > 0. \tag{9}$$

3.3. Constraint Eq.(4d)

For the sensitivity constraint, following method is used to obtain LMI form [18].

$$|W_pS| < 1 \Leftrightarrow \left|\frac{0.5s+\omega_p}{s}D\right| < |D+N(j\omega)|. \quad (10)$$

Square on (10) both sides and turn this inequality into matrix inequality form by using Schur Complement.

$$\begin{aligned} &\left|\frac{0.5s+\omega_p}{s}\right|^2\left|\frac{D}{s}\right|^2 < \left|\frac{D+N(j\omega)}{s}\right|^2 \\ &\Leftrightarrow \begin{bmatrix} \frac{1}{\left|\frac{D}{s}\right|^2} & \frac{0.5s+\omega_p}{s} \\ (\frac{0.5s+\omega_p}{s})^* & \left|\frac{D+N}{s}\right|^2 \end{bmatrix} > 0 \qquad (11) \\ &= \begin{bmatrix} S_{11} & S_{12} \\ (S_{12})^* & S_{22} \end{bmatrix} > 0. \end{aligned}$$

S_{11} and S_{22} still need to be transformed into linear function of variables. For S_{11},

$$\begin{aligned} S_{11} &= \frac{1}{|(s\tau^2+2k\tau)|^2} = \frac{1}{\omega^2\tau^4+4k^2\tau^2} \\ &\geq \frac{1}{\omega^2\tau_i^2\tau_{(i-1)}^2+4\tau_i^2} = \frac{1}{(\omega^2\tau_{(i-1)}^2+4)}\frac{1}{\tau_i^2}. \end{aligned} \quad (12)$$

τ_i^{-2} still needs to be dealt with. By using the following technique, the lower bound of τ_i^{-2} can be obtained .

$$\begin{aligned} &(\tau_i^{-2}-\tau_{i-1}^{-2})(\tau_i^{-2}-\tau_{i-1}^{-2}) \geq 0 \\ &\Leftrightarrow \tau_i^{-4} \geq 2\tau_{i-1}^{-2}\tau_i^{-2}-\tau_{i-1}^{-4} \Leftrightarrow \tau_i^{-2} \geq 2\tau_{i-1}^{-2}-\tau_{i-1}^{-4}\tau_i^2. \end{aligned} \quad (13)$$

By introducing a new variable ϕ_1 and making $2\tau_{i-1}^{-2} - \tau_{i-1}^{-4}\tau_i^2 > \phi_1 > 0$, LMI form constraint can be obtained.

$$\begin{bmatrix} 2\tau_{i-1}^2-\phi_1\tau_{i-1}^4 & \tau_i \\ \tau_i & 1 \end{bmatrix} > 0, \phi_1 > 0. \quad (14)$$

In conclusion. S_{11} part can be transformed into

$$S_{11} = \frac{1}{\left|\frac{D}{s}\right|^2} \geq \frac{1}{(\omega^2\tau_{(i-1)}^2+4)}\phi_1. \quad (15)$$

As for S_{22}, the linear approximation was employed. Let $\frac{N(j\omega)}{s} = x_k + y_kj$,

$$\begin{aligned} S_{22(i)} &= \left\|(s\tau_i^2+2k_i\tau_i)+(x_k+y_kj)\right\|^2 \\ &= S_{22(i-1)} + S'_{22(\tau,i-1)}(\tau_i-\tau_{i-1}) \\ &+ S'_{22(k,i-1)}(k_i-k_{i-1}) = \Phi, \end{aligned} \quad (16)$$

in which

$$S_{22(i-1)} = \left\|(s\tau_{i-1}^2+2k_{i-1}\tau_{i-1})+(x_k+y_kj)\right\|^2, \quad (17a)$$

$$\begin{aligned} S'_{22(\tau,i-1)} &= 4\omega\tau_{i-1}(\tau_{i-1}^2\omega+y_k) \\ &+ 4k_{i-1}(2k_{i-1}\tau_{i-1}+x_k), \end{aligned} \quad (17b)$$

$$S'_{22(k,i-1)} = 4\tau_{i-1}(2k_{i-1}\tau_{i-1}+x_k). \quad (17c)$$

In summary, the original nonlinear constraint (4d) can be transformed into the following LMIs by combining (11), (12), (14), and (16).

$$\begin{bmatrix} \frac{1}{(\omega^2\tau_{(i-1)}^2+4)}\phi_1 & \frac{0.5s+\omega_p}{s} \\ (\frac{0.5s+\omega_p}{s})^* & \Phi \end{bmatrix} > 0, \quad (18a)$$

$$\begin{bmatrix} 2\tau_{i-1}^2-\phi_1\tau_{i-1}^4 & \tau_i \\ \tau_i & 1 \end{bmatrix} > 0,\ \phi_1 > 0. \quad (18b)$$

3.4. Constraint Eq. (4e)

For complementary sensitivity constraint, by following similar process as dealing with previous one, the desired LMI form constraint can be obtained.

$$|W_mT| < 1 \Leftrightarrow \left|\frac{s+\omega_t}{1.25\omega_t}\right| < \left|\frac{D+N(j\omega)}{N(j\omega)}\right|. \quad (19)$$

After squaring both sides and using Schur Complement, the following results can be developed.

$$\begin{aligned} &\left|\frac{s+\omega_t}{1.25\omega_t}\right|^2 < \left|\frac{D+N(j\omega)}{N(j\omega)}\right|^2, \\ &\Leftrightarrow \frac{|s+\omega_t|^2\left|\frac{N(j\omega)}{s}\right|^2}{|1.25\omega_t|^2} < \left|\frac{D+N(j\omega)}{s}\right|^2, \\ &\Leftrightarrow \begin{bmatrix} |\omega_t|^2 & \frac{\left|\frac{N(j\omega)}{s}\right|(s+\omega_t)}{1.25} \\ \frac{(\left|\frac{N(j\omega)}{s}\right|(s+\omega_t))^*}{1.25} & \left|\frac{D+N(j\omega)}{s}\right|^2 \end{bmatrix} > 0, \\ &= \begin{bmatrix} T_{11} & T_{12} \\ (T_{12})^* & T_{22} \end{bmatrix} > 0. \end{aligned} \quad (20)$$

As before, T_{11} and T_{22} needs transformation. Since $T_{22} = S_{22}$, this part is omitted due to the repeatence. For T_{11}, the linear approximation is used.

$$\omega_{t(i)}^2 \geq 2\omega_{t(i-1)}\omega_{t(i)} - \omega_{t(i-1)}^2, \quad (21)$$

in which $\omega_{t(i)}$ is the current value while $\omega_{t(i-1)}$ represents for the previous one in optimization loop.

Combining (16), (20) and (21), the original nonlinear constraint (4e) can be changed into

$$\begin{bmatrix} 2\omega_{t(i-1)}\omega_{t(i)}-\omega_{t(i-1)}^2 & \frac{\left|\frac{N(j\omega)}{s}\right|(s+\omega_{t(i)})}{1.25} \\ \frac{(\left|\frac{N(j\omega)}{s}\right|(s+\omega_{t(i)}))^*}{1.25} & \Phi \end{bmatrix} > 0. \quad (22)$$

3.5. Constraints summary

After finishing all the process mentioned above, the original constraints have been formulated into a new form as follows.

$$\underset{\tau,k,\omega_t,\phi_1}{\text{Maximise}} \quad \omega_p \tag{23a}$$

$$\text{Subject to } \omega_p > 0, \phi_1 > 0, \omega_p < \frac{-\tau_i}{\tau_{i-1}^2} + \frac{2}{\tau_{i-1}}, \tag{23b}$$

$$0.5 < k < 1, \begin{bmatrix} 2\tau_{i-1}^2 - \phi_1 \tau_{i-1}^4 & \tau_i \\ \tau_i & 1 \end{bmatrix} > 0, \tag{23c}$$

$$\begin{bmatrix} \omega_t & 1 \\ 1 & \tau \end{bmatrix} > 0, \begin{bmatrix} \frac{1}{(\omega^2\tau_{(i-1)}^2 + 4)}\phi_1 & \frac{0.5s+\omega_p}{s} \\ (\frac{0.5s+\omega_p}{s})^* & \Phi \end{bmatrix} > 0, \tag{23d}$$

$$\begin{bmatrix} 2\omega_{t(i-1)}\omega_{t(i)} - \omega_{t(i-1)}^2 & \frac{\left|\frac{N(j\omega)}{s}\right|(s+\omega_{t(i)})}{1.25} \\ \frac{(\left|\frac{N(j\omega)}{s}\right|(s+\omega_{t(i)}))^*}{1.25} & \Phi \end{bmatrix} > 0 \tag{23e}$$

By finishing the reformulation of the problem, the optimization problem has been changed in to a convex optimization problem and can be solved by commercial solvers, for instance yalmip plus Mosek[19][20] in Matlab.

4. SIMULATION RESULT AND ANALYSIS

4.1. Simulation plant

In this paper, the Bode plot of nominal plant P_n(2nd order transfer function) and actual real plant $P_r(j\omega)$(frequency response data) is shown in Fig. 2. The nominal plant catches the dynamics of real plant in less than 10Hz frequency range and doesn't contain unstable zeros.

$$P_n = \frac{84.977}{s(s+2.101)}, Q = \frac{1}{\tau^2 s^2 + 2k\tau s + 1}, \tag{24a}$$

$$L = \frac{(s+2.101)}{84.977(s\tau^2 + 2k\tau)} P_r(j\omega), \tag{24b}$$

$$S = \frac{84.977(s\tau^2 + 2k\tau)}{84.977(s\tau^2 + 2k\tau) + P_r(j\omega)(s+2.101)}, \tag{24c}$$

$$T = \frac{P_r(j\omega)(s+2.101)}{84.977(s\tau^2 + 2k\tau) + P_r(j\omega)(s+2.101)}. \tag{24d}$$

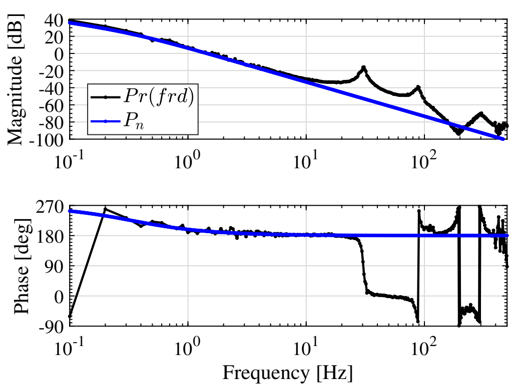

Fig. 2 Bode plot of real plant(frd) and nominal plant

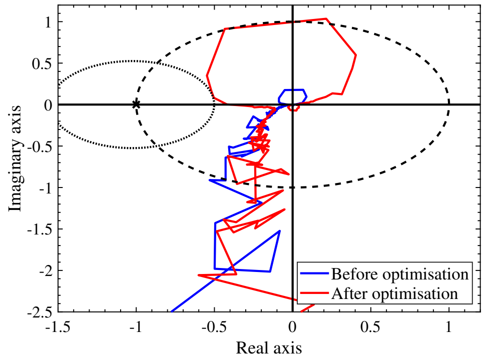

Fig. 3 Nyquist plot of before and after optimization

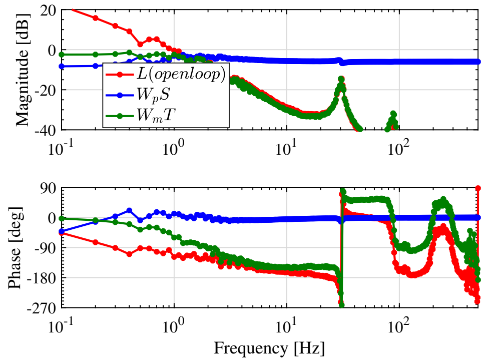

Fig. 4 Bode plot of open loop function L, W_pS and W_mT before optimization

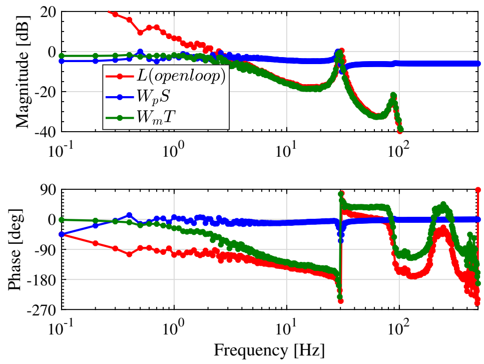

Fig. 5 Bode plot of open loop function L, W_pS and W_mT after optimization

4.2. Case study result

In this section, by building the constraints following the proposed method, the ω_p can be maximized. The simulation initial condition is given as $\tau_{init} = 0.1$ [s], $k_{init} = 0.9$, $\omega_{p(init)} = \pi$ [rad/s], $\omega_{t(init)} = 80\pi$ [rad/s].

After using convex optimization, $\tau_{opt} = 0.0419$ [s], $k_{opt} = 1$, $\omega_{p(opt)} = 9.9$ [rad/s]. In Fig. 3, dashed black line represents for unit circle and dotted black line is a circle whose center locates at (-0.5,0) and the radius is 0.5. Since the closest distance from Nyquist plot to critical point $(-1, 0)$ is modulus margin (the inverse of the maximum of the sensitivity function), Nyquist plot has no intersection with dashed circle implies that the sensitivity function constraint holds successfully. And proposed optimization method makes the Nyquist plot become tangent to the dashed circle. The predefined peak value con-

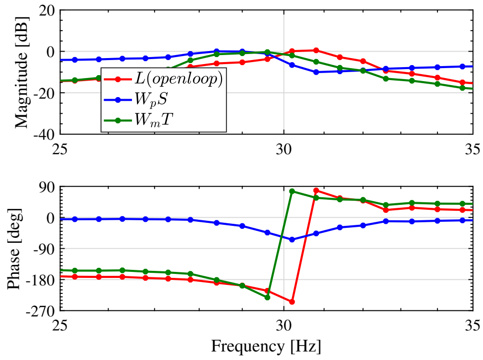

Fig. 6 Locally enlarged figure of Fig. 5

straints for S and T have been satisfied can also be told more straightforwardly from Fig. 5 and Fig. 6 in which $|W_pS|$ and $|W_mT|$ are always under 0 dB.

4.3. Disturbance rejection performance

Simulations also have been done to test the disturbance rejection performance after using designed Q filter in Fig. 7. During this simulation, a well-identified transfer function (tf) of P_r(8th order) (as shown in Fig. 8) was used and feedback controller $C_{fb}$was chosen as follows.

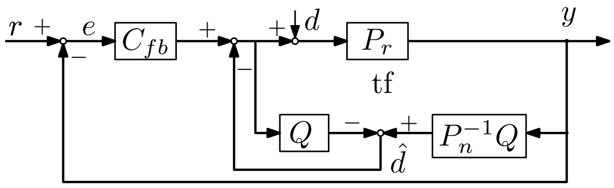

Fig. 7 Block diagram of disturbance observer control system

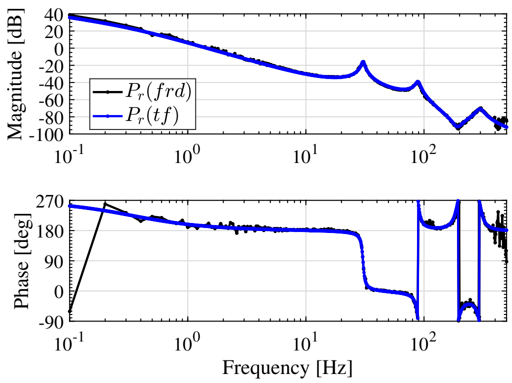

Fig. 8 Bode plot of P_r (8th order transfer function) and P_r (frequency response data)

$$C_{fb} = 1.36 + \frac{3.64}{s} + \frac{0.261s}{0.0249s+1}. \tag{25}$$

Making reference input as zero and injecting unit step disturbance to the system, the output response are shown in Fig. 9. The proposed Q filter design outperforms initial Q filter and disturbance rejection performance has been improved.

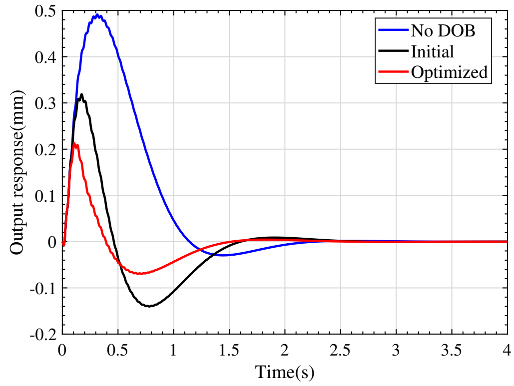

Fig. 9 Output response when initial Q filter and optimized Q filter are employed

5. CONCLUDING REMARKS

5.1. Conclusion

This paper has proposed a novel optimization method for maximizing bandwidth of disturbance observer configuration by just using frequency response data. What's more, all the nonlinear constraints are transformed into convex form which can be solved by convex optimization method. The simulation results verify the feasibility of proposed method.

5.2. Analysis and Future work

In this paper, two parameters of Q filter has been tuned. Although the real plant is a non-minimum phase one, the nominal plant in this paper is a second order minimum phase one. In the future, proposed method will be extended to the design of DOB system when non-minimum phase nominal plant is involved.

6. ACKNOWLEDGMENT

The work is supported by JSPS KAKENHI Grant Number 18H05902 and the Telecommunications Advancement Foundation. The student is supported by China Scholarship Council (CSC). The authors thank Professor Hiroshi Fujimoto (The University of Tokyo) cordially for providing the frequency data.

REFERENCES

[1] K. Ohishi, K. Ohnishi, and K. Miyachi, "Torque-speed regulation of DC motor based on load torque estimation method ", *International Power Electronics Conference*, pp. 1209–1218, 1983.

[2] E. Schrijver and J. van Dijk, "Disturbance observers for rigid mechanical systems: equivalence, stability, and design", *Journal of Dynamic Systems, Measurement, and Control*, vol. 124, no. 4, pp. 539-548, 2002.

[3] S. Endo, H. Kobayashi, C. J. Kempf, S. Kobayashi, M. Tomizuka, and Y. Hori, "Robust digital tracking controller design for high-speed positioning systems", *Control Enigineering Practice*, vol. 4, no. 4, pp. 527–536, 1996.

[4] K. Ohnishi, M. Shibata, and T. Murakami, "Motion control for advanced mechatronics", *IEEE/ASME Transactions on Mechatronics*, vol. 1, no. 1, pp. 56–67, 1996.
[5] E. Sariyildiz and K. Ohnishi, "A new solution for the robust control problem of non-minimum phase systems using disturbance observer", *IEEE International Conference on Mechatronics*, pp. 46–51, 2013.
[6] X. Chen and M. Tomizuka, "Optimal plant shaping for high bandwidth disturbance rejection in discrete disturbance observers", *Proceedings of the American Control Conference*, pp. 2641–2646, 2010.
[7] H. Shim and Y. J. Joo, "State space analysis of disturbance observer and a robust stability condition", *Proceedings of the IEEE Conference on Decision and Control*, pp. 2193–2198, 2007.
[8] C. C. Wang and M. Tomizuka, "Design of robustly stable disturbance observers based on closed loop consideration using H_∞ optimization and its applications to motion control systems", *Proceedings of the American Control Conference*, pp. 3764–3769, 2004.
[9] E. Sariyildiz and K. Ohnishi, "A Guide to design disturbance observer", *Journal of Dynamic Systems, Measurement, and Control*, vol. 136, no. 2, 2014.
[10] H. Shim, N. H. Jo and Y. Son, "A new disturbance observer for non-minimum phase linear systems", *Proceedings of the American Control Conference*, pp. 3385-3389, 2008.
[11] A. Karimi, M. Kunze, and R. Longchamp, "Robust controller design by linear programming with application to a double-axis positioning system", *Control Engineering Practice*, vol. 15, no. 2, pp. 197–208, 2007.
[12] A. J. Den Hamer, S. Weiland, and M. Steinbuch, "Model-free norm-based fixed structure controller synthesis", *Proceedings of the IEEE Conference on Decision and Control*, pp. 4030–4035, 2009.
[13] A. Karimi and G. Galdos, "Fixed-order H_∞ controller design for nonparametric models by convex optimization", *Automatica*, vol. 46, no. 8, pp. 1388–1394, 2010.
[14] M. Hast, K. J. Åström, B. Bernhardsson, and S. Boyd, "PID design by convex-concave optimization ", *Proceedings of the European Control Conference*, pp. 4460–4465, 2013.
[15] K. Nakamura, K. Yubai, D. Yashiro, and S. Komada, "Controller design method achieving maximization of control bandwidth by using Nyquist diagram ", *Proceedings of the International Automatic Control Conference*, pp. 35–40, 2016.
[16] G. Galdos, A. Karimi, and R. Longchamp, "H_∞ controller design for spectral MIMO models by convex optimization" , *Journal of Process Control*, vol. 20, no. 10, pp. 1175-1182, 2010.
[17] A. Karimi, "Frequency-domain robust control toolbox " , *Proceedings of the IEEE Conference on Decision and Control*, pp. 3744-3749, 2013.
[18] K. Nakamura, K. Yubai, D. Yashiro and S. Komada, "Fully parameterized controller design method for high control bandwidth using frequency response data sets ", *Proceedings of the International Workshop on Sensing Actuation, and Motion Control*, 2017.
[19] J. Löfberg, "YALMIP : a toolbox for modeling and optimization in MATLAB", *IEEE International Conference on Robotics and Automation*, pp. 284-289, 2004
[20] MOSEK ApS, "MOSEK optimization toolbox for MATLAB manual", 2019.